Article:

Wang, S., Zhao, L., Liang, K. et al. (2 more authors) (2018) Energy beamforming for full-duplex wireless-powered communication networks. Physical Communication, 26. ISSN 1874-4907

https://doi.org/10.1016/j.phycom.2017.12.007

Energy Beamforming for Full-Duplex Wireless-Powered Communication Networks

Shuai Wang[a], Liqiang Zhao[a,*], Kai Liang[a], Xiaoli Chu[b], Bingli Jiao[c]

[a]*State Key Laboratory of Integrated Services Networks, Xidian University, Xi'an 710071, China*
[b]*Dept. of Electronic and Electrical Engineering, University of Sheffield, Sheffield, S1 3JD, UK*
[c]*School of Electronics Engineering and Computer Science, Peking University, Beijing 100871, China*

Abstract

In this paper, we consider a full-duplex (FD) wireless-powered communication network (WPCN), where one FD hybrid access point (HAP) equipped with multiple antennas simultaneously transmits energy to and receives information from multiple users. Firstly, we propose a space division wireless energy allocation scheme and calculate the harvested energy in downlink wireless energy transfer (WET) for each user. Secondly, we derive an approximate closed-form expression of user's achievable ergodic rate in uplink wireless information transfer (WIT). Thirdly, the energy allocation for different users is optimized under the max-min user fairness constraint, and a closed-form solution is obtained. Numerical results show that the simulation and the approximation of achievable rates are well matched, and energy beamforming can effectively suppress self-interference (SI), and improve rates as well as fairness among users. Moreover, FD-WPCNs are shown to outperform half-duplex (HD) WPCNs in rates with same number of antennas.

Keywords: Full-duplex, fairness, power allocation, wireless-powered communication networks, beamforming

1. Introduction

Nowadays, the performance of wireless devices are severely restricted by finite battery capacity. To prolong the lifetime of smart devices in wireless sensor networks (WSNs) and Internet of things (IoTs), we investigate wireless-powered communication networks (WPCNs) [1, 2], where user equipment uses energy harvested from radio frequency (RF) signals to transmit information.

Full-duplex (FD) transmission is a potential technology for 5G communications. To improve the utilization of time and spectrum resources, FD technique has been investigated in multi-user WPCNs. In FD-WPCNs, hybrid information and energy access points (HAPs) simultaneously transmit energy and receive information, and users can keep on harvesting energy when other users are transmitting information, while in most exiting works on WPCNs, HAPs operate in the half-duplex (HD) mode [3, 4, 5, 6, 7]. Multi-user FD-WPCN models considering single transmit block with energy causality were proposed in [8, 9]. In [10], authors studied the optimal resource allocation of multi-user FD-WPCNs.

However, in [8, 9, 10], all the HAPs are equipped with only two antennas, one for wireless energy transfer (WET) and the other for wireless information transfer (WIT), and the resource allocation is achieved by adjusting the transmission time allocated to users. Multi-antenna can suppress self-interference (SI), which seriously affects the performance of FD system [11]. Upon invoking the advantages of multiple antennas, we adopt energy beamforming to allocate energy for different users through space division multiple access (SDMA). In [12], authors discussed full-duplex wireless-powered MIMO systems consisting of one multi-antenna HAP and one multi-antenna user, while our system including multiple single-antenna users.

Energy beamforming in simultaneous wireless information and power transfer (SWIPT) system was investigated in [13], and a novel energy borrowing technique was put forward in [14], in which energy harvesting nodes borrowed energy from the power grid and returned the energy back with additional energy interest. In a WPCN, users with poor channels harvest less energy in WET while they need more transmit power to overcome fading in uplink WIT, which causes the performance gap among users, a.k.a., the doubly near-far problem [1]. To ensure the fairness among users, in [3, 4], HAPs allocate more power to users with poor channels by energy beamforming.

Taking user fairness into account, we investigate the effects of energy beamforming on FD-WPCNs. In this paper, we firstly propose an improved FD-WPCN model by equipping two groups of antennas on HAPs for downlink WET and uplink WIT, respectively. Secondly, we consider a space division energy allocation scheme using energy beamforming, and derive users' harvested energy. Thirdly, the approximate close-form expression of each user's achievable ergodic rate is derived to show the effects of residual SI and the number of antennas. Further, We derive a closed-form energy allocation solution under the max-min user fairness constraint. Finally, through numerical results, we verify that the approximation of rates is well matched with the simulation results. Numerical results also

*Corresponding author

Email addresses: wangshuaixidian@yeah.net (Shuai Wang), lqzhao@mail.xidian.edu.cn (Liqiang Zhao), kliang@xidian.edu.cn (Kai Liang), x.chu@sheffield.ac.uk (Xiaoli Chu), jiaobl@pku.edu.cn (Bingli Jiao)

show that exploiting energy beamforming in FD-WPCN provides the following benefits: 1) improving overall rates of FD-WPCNs; 2)ensuring fairness among users; 3) Suppressing SI. Moreover, under a realizable SI cancellation, FD-WPCNs are shown to outperform HD-WPCNs in rates with same number of antennas.

The rest of this paper is organized as follows. Section 2 introduces the FD-WPCN model and formulates the optimization problem. Section 3 presents the approximation and analysis of achievable ergodic rates. In section 4, we optimize the power allocation. Numerical results and conclusion are given in Section 5 and Section 6, respectively.

Notations: Lower and upper case boldfaced letters represent vectors and matrices, respectively. $\mathbb{C}^{X\times Y}$ denotes a $X\times Y$ complex valued matrices. The Euclidean norm, the variance and the expectation are denoted by $\|\cdot\|_2$,$Var[\cdot]$and $\mathbb{E}[\cdot]$, respectively. $\mathbf{H}^H$ denotes the Hermitian of matrix $\mathbf{H}$. $\mathcal{CN}(0,\sigma^2)$ denotes the set of complex Gaussian variables with zero mean and covariance σ^2.

2. System Model and Problem Formulation

2.1. System model and block structure

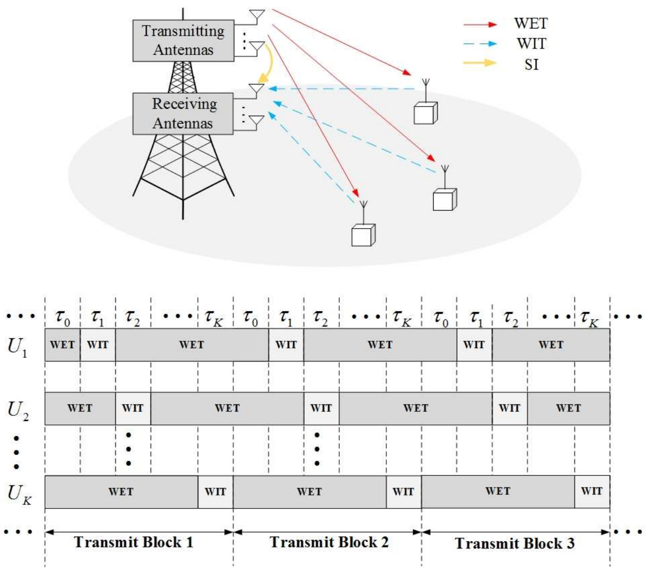

Figure 1: System model and structure of transmit block

We consider a multi-user FD-WPCN, where a FD HAP simultaneously transmits energy to and receive information from K single-antenna users (denoted by U_k, $k=1,\cdots,K$) by employing N_t transmitting antennas and N_r receiving antennas, as shown in Fig. 1. All users operate in the time division duplex (TDD) mode over the same frequency band. Assume that the users can only harvest energy from the HAP and then use the harvested energy to transmit information in the uplink.

Fig. 1 also shows the transmit block structure of the system. In traditional WPCNs, one block is usually divided into two phases for WET and WIT, respectively. However, in our proposed FD model, one block of duration T is divided into $K+1$ time slices denoted by τ_k, $i=0,1,\cdots,K$. We assume that all time slices are of the same duration, i.e. $\forall k$, $\tau_k = T/(K+1)=\tau$. Without loss of generality, we assume $T=1$. User U_k transmits information in the kth slice and harvests energy in the other K slices. In addition, the 0th slice is a dedicated WET slice, which ensures the system working properly even with only one user [10]. What should be noted is that in [8, 9], users stop harvesting energy after WIT phase considering single transmit block and energy causality, while in our FD model, users harvest energy after the WIT phase and use the harvested energy for information transfer in next block, thus avoiding wasting energy.

In the FD-WPCN, the HAP employs multi-antenna technology to communicate with single-antenna users. We define $\mathbf{G}_d^H\in\mathbb{C}^{K\times N_t}$ and $\mathbf{G}_u\in\mathbb{C}^{N_r\times K}$ as the channel matrices from the HAP's transmitting antennas to the K users, and from the K users to the HAP's receiving antennas, respectively. We can express $\mathbf{G}_d$ and $\mathbf{G}_u$ as $\mathbf{G}_d=\mathbf{H}_d\mathbf{D}_d^{1/2}$ and $\mathbf{G}_u=\mathbf{H}_u\mathbf{D}_u^{1/2}$, where $\mathbf{H}_d^H\in\mathbb{C}^{K\times N_t}$ and $\mathbf{H}_u\in\mathbb{C}^{N_r\times K}$ are the small-scale fading matrices and have i.i.d. $\mathcal{CN}(0,1)$ elements. Here $\mathbf{g}_{d,k}$, $\mathbf{g}_{u,k}$, $\mathbf{h}_{d,k}$ and $\mathbf{h}_{u,k}$ denote the kth column of $\mathbf{G}_d$, $\mathbf{G}_u$, $\mathbf{H}_d$ and $\mathbf{H}_u$, respectively. $\mathbf{D}_d$ and $\mathbf{D}_u$ are K order diagonal matrices with $[\mathbf{D}_d]_{kk}=\beta_{d,k}$ and $[\mathbf{D}_u]_{kk}=\beta_{u,k}$, respectively. Here, $\beta_{d,k}$ and $\beta_{u,k}$ represent downlink and uplink large-scale fading coefficients, respectively. All users send pilot sequences L to the FD HAP before the beginning of their energy transfer. By exploiting those pilot sequences, the FD HAP estimates the uplink and downlink channel matrices as $\widehat{\mathbf{G}_\mathbf{d}}$ and $\widehat{\mathbf{G}_\mathbf{u}}$, respectively. Here we assume perfect channel estimation, i.e. $\widehat{\mathbf{G}_\mathbf{d}}=\mathbf{G}_d$, $\widehat{\mathbf{G}_\mathbf{u}}=\mathbf{G}_u$.

In a FD-WPCN system, the HAP's transmit power is much greater than the power of the received signal at HAP, which will cause serious SI. Since transmitting antennas are close to receiving antennas, the propagation delay is small. Therefore, the SI signal's light-of-sight component can be efficiently reduced by RF domain self-interference cancellation (SIC) technology [11]. As a result, the residual SI channel denoted by $\mathbf{G}_s\in\mathbb{C}^{N_t\times N_r}$ is assumed as Rayleigh fading [11] and the elements of $\mathbf{G}_s$ are i.i.d. following $\mathcal{CN}(0,\sigma_s^2)$, where σ_s^2 is defined as the SIC capability of FD-WPCN system.

2.2. Downlink wireless energy transfer

The energy that U_k uses for WIT is harvested from last transmit block's $(k+1)$th time slice to current transmit block's $(k-1)$th time slice. Since users do not need to demodulate the WET signal, we assume that all users share the same symbol x_d in WET with $|x_d|=1$. The received signal over the downlink at U_k during τ_j, $k\neq j$ denoted by $y_{d,k}$, is given by

$$y_{d,k}=\sqrt{P_d}\mathbf{g}_{d,k}^H\mathbf{w}(\mathbf{G}_d)x_d+n_{d,k}, \tag{1}$$

where P_d is the HAP's downlink transmit power, and $\mathbf{w}(\mathbf{G}_d)$ is given by

$$\mathbf{w}(\mathbf{G}_d)=\sum_{k=1}^{K}\sqrt{\alpha_k}\frac{\mathbf{g}_{d,k}}{\|\mathbf{g}_{d,k}\|_2}, \tag{2}$$

where α_k, the kth element of $\boldsymbol{\alpha}$, represents the power allocation weight for U_k, satisfying $\sum_{k=1}^{K}\alpha_k=1$.

In (1) and (2), $\mathbf{w}(\mathbf{G}_d)$ is the $N_t \times 1$ beamformer vector. The HAP broadcasts energy to all users with K energy beams to facilitate efficient energy transmission with the aid of energy beamforming. The beamforming vector is generated based on the downlink channel state $\mathbf{G}_d$, and has been proved asymptotical optimal for energy transfer [4].

Assume that the energy harvested from ambient noise and other users' uplink WIT signals can be neglected. Thus, the expected energy harvested by U_k in any slice $\tau_i, i \neq k$, can be expressed as

$$e_k = \eta \mathbb{E}[|\sqrt{P_d}\mathbf{g}_{d,k}^H \mathbf{w}(\mathbf{G}_d)|^2]\tau, \tag{3}$$

where $0 < \eta < 1$ is the energy converting efficiency at users.

For analytical simplicity, we assume that the large-scale fading coefficient $\beta_{d,k}$ are constant over blocks. Hence each user's expected harvested energy per slice denoted by e_k, which depends on $\beta_{d,k}$, is constant. Each user harvests energy during K time slices before WIT phase, the expected energy stored for $U_k's$ WIT, which is denoted as E_k, can be expressed as

$$\begin{aligned} E_k &= \sum_{i=1, i\neq k}^{K} e_i \\ &= \eta \mathbb{E}[|\sqrt{P_d}\mathbf{g}_{d,k}^H \mathbf{w}(\mathbf{G}_d)|^2]\tau K. \end{aligned} \tag{4}$$

2.3. Uplink wireless information transfer

During the kth time slice, U_k transmits information to the HAP using the energy harvested in WET slices. The received signal at HAP over the uplink during τ_k is given by

$$\mathbf{y}_{u,k} = \sqrt{P_{u,k}}\mathbf{g}_{u,k}x_{u,k} + \sqrt{P_d}\mathbf{G}_s^H \mathbf{w}(\mathbf{G}_d)x_d + \mathbf{n}_{u,k}, \tag{5}$$

where $x_{u,k}$ is the signal transmitted by U_k during τ_k, satisfying $x_{u,k} \sim \mathcal{CN}(0,1)$. $\mathbf{n}_{u,k}$ is the $N_r \times 1$ noise vector at HAP and its elements follows i.i.d $\mathcal{CN}(0, \sigma^2)$.

Since TDD transmission model is adopted, the HAP adopts a maximal ratio combining (MRC) for the uplink information reception. The detected signal denoted by $r_{u,k}$ is given by

$$\begin{aligned} r_{u,k} &= \mathbf{g}_{u,k}^H \mathbf{y}_{u,k} \\ &= \sqrt{P_{u,k}}\mathbf{g}_{u,k}^H \mathbf{g}_{u,k} x_{u,k} + \mathbf{g}_{u,k}^H \mathbf{n}_{u,k} \\ &\quad + \sqrt{P_d}\mathbf{g}_{u,k}^H \mathbf{G}_s^H \mathbf{w}(\mathbf{G}_d)x_d, \end{aligned} \tag{6}$$

where the third term indicates the SI. From (6), we can derive the achievable ergodic rate of U_k, and then the sum achievable rate of the FD-WPCN system.

2.4. Problem formulation

Under the max-min criterion, we formulate the optimization problem to find the fair power allocation among users by optimizing over the power allocation weights $\boldsymbol{\alpha}$.

Considering the fairness among users, the following optimization problem is formulated to maximize the minimum rate among all users.

$$\begin{aligned} (P_1): \quad & \max_{\alpha} \min_{k} \quad R_k \quad k \in 1, \cdots, K, \\ & \text{subject to} \quad \sum_{k=1}^{K} \alpha_k = 1, \\ & \qquad\qquad \alpha_k \geq 0, \quad \forall k \in 1, \cdots, K, \end{aligned}$$

where the achievable ergodic rate of U_k is denoted by R_k.

Generally, R_k is decided by harvested energy, as well as channel state and the number of receiving antennas. However, in FD-WPCN, SI must be considered, which will be analyzed in Section 3.

3. Achievable Ergodic Rate for FD-WPCN

In this section, we derive the expected harvested energy in downlink WET phase and the achievable ergodic rates in uplink WIT phase. After that, we analyze the effects of SI and the number of antennas on overall rates.

The uplink WIT achievable rate is correlated with its uplink transmit power, so we first derive U_k's expected transmit power denoted by $P_{u,k}$, which is given by the following lemma.

Lemma 1. *The expected transmit power of U_k is*

$$P_{u,k} = \eta P_d \beta_{d,k}[(N_t - 1)\alpha_k + 1]K. \tag{7}$$

Proof of Lemma 1. From (3), $P_{u,k}$ can be expressed as

$$P_{u,k} = E_{u,k}/\tau_k = \eta P_d \mathbb{E}[|\mathbf{g}_{d,k}^H \mathbf{w}(\mathbf{G}_d)|^2]K, \tag{8}$$

where we denote $\mathbb{E}[|\mathbf{g}_{d,k}^H \mathbf{w}(\mathbf{G}_d)|^2]$ as ϕ_k, which is computed as

$$\begin{aligned} \phi_k &= \mathbb{E}[|\mathbf{g}_{d,k}^H \sum_{k=1}^{K} \sqrt{\alpha_k}\frac{\mathbf{g}_{d,k}}{||\mathbf{g}_{d,k}||_2}|^2] \\ &= \alpha_k \mathbb{E}[|\mathbf{g}_{d,k}^H \frac{\mathbf{g}_{d,k}}{||\mathbf{g}_{d,k}||_2}|^2] + \sum_{i\neq k}^{K} \alpha_i \mathbb{E}[|\mathbf{g}_{d,k}^H \frac{\mathbf{g}_{d,i}}{||\mathbf{g}_{d,i}||_2}|^2] \\ &\quad + \sum_{i\neq k}^{K}\sum_{j\neq k,i}^{K} \sqrt{\alpha_i}\sqrt{\alpha_j}\mathbb{E}[\mathbf{g}_{d,k}^H \frac{\mathbf{g}_{d,i}}{||\mathbf{g}_{d,i}||_2}\frac{\mathbf{g}_{d,j}^H}{||\mathbf{g}_{d,j}||_2}\mathbf{g}_{d,k}] \\ &\overset{(a)}{=} \alpha_k \beta_{d,k}\mathbb{E}[|\mathbf{h}_{d,k}^H \frac{\mathbf{h}_{d,k}}{||\mathbf{h}_{d,k}||_2}|^2] + \sum_{i\neq k}^{K} \alpha_i \beta_{d,k}\mathbb{E}[|\mathbf{h}_{d,k}^H \frac{\mathbf{h}_{d,i}}{||\mathbf{h}_{d,i}||_2}|^2], \end{aligned} \tag{9}$$

where (a) holds because $g_{d,i}$ is uncorrelated with $\mathbf{g}_{d,j}$ for any $i \neq j$. Each $\mathbf{h}_{d,k}$ is an independent complex Gaussian random vector, according to [5, 15], the first and second terms of (9) follow gamma distribution shown as

$$\alpha_k \beta_{d,k}|\mathbf{h}_{d,k}^H \frac{\mathbf{h}_{d,k}}{||\mathbf{h}_{d,k}||_2}|^2 \sim \Gamma(N_t, \alpha_k \beta_{d,k}), \tag{10}$$

$$\alpha_i \beta_{d,k}|\mathbf{h}_{d,k}^H \frac{\mathbf{h}_{d,i}}{||\mathbf{h}_{d,i}||_2}|^2 \sim \Gamma(K, \frac{\alpha_i \beta_{d,k}}{K}), \tag{11}$$

where $\Gamma(\kappa,\theta)$ denotes gamma distribution with shape parameter κ and scale parameter θ, and $\mathbb{E}[\Gamma(\kappa,\theta)] = \kappa\theta$. Therefore, ϕ_k can be computed as

$$\phi_k = \beta_{d,k}(\alpha_k N_t + \sum_{i\neq k}^{K} \alpha_i). \tag{12}$$

Substituting ϕ_k into (8), we can obtain (7). □

Using Shannon's Theorem, the achievable ergodic rate of U_k can be expressed as

$$R_k = \tau\mathbb{E}[\log_2(1+\gamma_k)], \tag{13}$$

where γ_k is the signal-to-interference-plus-noise ratio (SINR) of U_k and can be expressed as

$$\gamma_k = \frac{P_{u,k}|\mathbf{g}_{u,k}^H \mathbf{g}_{u,k}|^2}{|\mathbf{g}_{u,k}^H \mathbf{n}_{u,k}|^2 + P_d|\mathbf{g}_{u,k}^H \mathbf{G}_s^H \mathbf{w}(\mathbf{G}_d)|^2}. \tag{14}$$

Similar to [4, 16], according to Jensen's inequality and the convexity of the function $\log_2(1+1/x)$, we can obtain one tight lower bound of R_k, denoted by $\widetilde{R}_k$, as

$$R_k \geq \widetilde{R}_k = \tau\log_2(1+\tilde{\gamma}_k), \tag{15}$$

where $\tilde{\gamma}_k$ is defined as

$$\tilde{\gamma}_k = \frac{1}{\mathbb{E}\left[\gamma_k^{-1}\right]}. \tag{16}$$

In Section 5, we will show that the lower bound matches well through simulation. By calculating $\widetilde{R}_k$, we can derive a tight approximate value of R_k in the following lemma and make use of it to analyse the performance of the system and derive an approximate optimal solution of (P_1).

Lemma 2. *The lower bound of R_k is given by*

$$\widetilde{R}_k = \tau\log_2(1+\frac{P_{u,k}\beta_{u,k}(N_r-1)(N_r-2)}{N_r(\sigma^2+P_d\sigma_s^2)}). \tag{17}$$

Proof of Lemma 2. Since the elements of $g_{u,k}$, $n_{u,k}$ and $\mathbf{G}_s$ are mutually independent, we can obtain $\tilde{\gamma}_k$ with

$$\begin{aligned}\mathbb{E}\left[\gamma_k^{-1}\right] &= \mathbb{E}\left[\frac{|\mathbf{g}_{u,k}^H\mathbf{n}_{u,k}|^2 + P_d|\mathbf{g}_{u,k}^H\mathbf{G}_s^H\mathbf{w}(\mathbf{G}_d)|^2}{P_{u,k}|\mathbf{g}_{u,k}^H\mathbf{g}_{u,k}|^2}\right]\\ &= \mathbb{E}\left[|\mathbf{g}_{u,k}^H\mathbf{n}_{u,k}|^2\right] + \mathbb{E}\left[P_d|\mathbf{g}_{u,k}^H\mathbf{G}_s^H\mathbf{w}(\mathbf{G}_d)|^2\right]\\ &\cdot\mathbb{E}\left[\frac{1}{P_{u,k}|\mathbf{g}_{u,k}^H\mathbf{g}_{u,k}|^2}\right]\\ &= \beta_{u,k}N_r(\sigma^2+P_d\sigma_s^2)\cdot\mathbb{E}\left[\frac{1}{P_{u,k}\beta_{u,k}^2|\mathbf{h}_{u,k}^H\mathbf{h}_{u,k}|^2}\right]. \end{aligned} \tag{18}$$

It's noticed that $2h_{u,k}^H h_{u,k}$ follows central chi-square distribution with the $2N_r$ degrees of freedom. Define $X = 2h_{u,k}^H h_{u,k}$, then $(1/X)$ follows inverse-chi-squared distribution [17], i.e. $(1/X) \sim \text{Inv-}\chi^2(2Nr)$. So it holds that

$$\begin{aligned}\mathbb{E}\left[\frac{1}{X^2}\right] &= \mathbb{E}\left[\frac{1}{4|\mathbf{h}_{u,k}^H\mathbf{h}_{u,k}|^2}\right]\\ &= Var\left[\frac{1}{X}\right] + \mathbb{E}^2\left[\frac{1}{X}\right]\\ &= \frac{2}{(2N_r-2)^2(2N_r-4)} + \frac{1}{(2N_r-2)^2}\\ &= \frac{1}{4(N_r-1)(N_r-2)}. \end{aligned} \tag{19}$$

Compute $\tilde{\gamma}_k$ with (18) and (19), then we can obtain (17). □

From Lemma 2, the power of SI and the detected signal at HAP, denoted by P_{SI} and P_{signal} respectively, are given by

$$P_{SI} = P_d N_r \beta_{u,k}\sigma_s^2, \tag{20}$$

$$P_{signal} = \eta P_d\beta_{d,k}[(N_t-1)\alpha_k+1]K\beta_{u,k}^2(N_r-1)(N_r-2). \tag{21}$$

Given that N_t and N_r are sufficiently large, we can see from (20) and (21) that P_{SI} is proportional to N_r and P_{signal} is proportional to $N_t N_r^2$. Therefore, the signal-to-interference ratio (SIR), which is the ratio between P_{signal} and P_{SI}, is proportional to $N_t\cdot N_r$. More specifically, along with the increasing number of antennas, the SIR increases and the influence of SI on rate performance can diminish.

For analytical convenience, $\tilde{\gamma}_k$ and $\widetilde{R}_k$ can be rewritten as

$$\tilde{\gamma}_k = AB_k[(N_t-1)\alpha_k+1], \tag{22}$$

$$\widetilde{R}_k = \tau\log_2(1+AB_k[(N_t-1)\alpha_k+1]), \tag{23}$$

where

$$A = \frac{\eta P_d K(N_r-1)(N_r-2)}{N_r(\sigma^2+P_d\sigma_s^2)}, \tag{24}$$

$$B_k = \beta_{u,k}\beta_{d,k}, \tag{25}$$

Assume that N_t and N_r are sufficiently large, and $\tilde{\gamma}_k > 1$. When $P_d \to \infty$, we can obtain one upper bound of $\widetilde{R}_k$ as

$$\lim_{P_d\to\infty}\widetilde{R}_k = \tau\log_2(1+\frac{\eta K N_r N_t B_k\alpha_k}{\sigma_s^2}), \tag{26}$$

which indicates that with residual SI, $\widetilde{R}_k$ will converge with the increasing of P_d, and the upper bound is decided by the SIC capability and number of antennas. Since there is no multi-user interference in the uplink, $\widetilde{R}_k$ will increase rapidly with better SIC capability.

4. Power Allocation

According to Lemma 2, the (P_1) can be recast as

$$\begin{aligned}(P_2):\quad &\max_{\alpha}\min_{k}\quad \widetilde{R}_k \quad k\in 1,\cdots,K,\\ &\text{subject to}\quad \sum_{k=1}^{K}\alpha_k = 1,\\ &\qquad\qquad \alpha_k \geq 0,\quad \forall k\in 1,\cdots,K.\end{aligned}$$

We obtain the closed-form solution of (P_2) as shown in the following theorem.

Theorem 1. *The optimal solution of* (P_2) *is given by*

$$\alpha_k = \frac{1}{N_t - 1}\left(\frac{N_t - 1 + K}{B_k \sum_{i=1}^{K} B_i^{-1}} - 1\right), \quad k \in 1, \cdots, K. \tag{27}$$

Proof of Theorem 1. Since the optimization problem (P_2) follows the max-min criterion, the average rate of each user should equal with rate of each other. Assuming that with any initial $\boldsymbol{\alpha}$ different from optimal weights, as long as there are difference in rate among users, the optimizer will increase the energy allocation weights of minimum-rate users while decreasing other's, until all users equal to each other. By converting (22), α_k can be written as

$$\alpha_k = \frac{\tilde{\gamma}_k - AB_k}{AB_k(N_t - 1)}. \tag{28}$$

Substitute (28) into $\sum_{k=1}^{K} \alpha_k = 1$ then we can obtain

$$\sum_{k=1}^{K} \frac{\tilde{\gamma}_k - AB_k}{AB_k(N_t - 1)} = 1. \tag{29}$$

Since all the $\tilde{\gamma}_k$ are equal, converting (29), $\tilde{\gamma}_k$ can be written as

$$\tilde{\gamma}_k = \frac{A(N_t - 1 + K)}{\sum_{i=1}^{K} B_i^{-1}}. \tag{30}$$

Substituting (30) into (28), we can obtain (27). □

Substituting the wights $\boldsymbol{\alpha}$ derived in Theorem 1 into (23), $\widetilde{R}_k$ can be expressed as

$$\widetilde{R}_k = \tau \log_2\left(1 + \frac{A(N_t - 1 + K)}{\sum_{i=1}^{K} B_i^{-1}}\right), \quad k \in 1, \cdots, K. \tag{31}$$

where the result shows that any user's rate equals to each other's. In other words, with Theorem 1, we achieve the fairness among users.

5. Numerical Results

In this section, we verify the performance of proposed FD-WPCN. In all illustrative results below, the distance between U_k and HAP denoted by D_k uniformly distributes within [5m,10m] for any U_k. In addition, we use the long-term fading model with $\beta_{u,k} = \beta_{d,k} = 10^{-3} D_k^{-\nu}$ where the pathloss exponent is set as $\nu = 2$. The noise at HAP is assumed to be -100 dBm/Hz. For all users, it's assumed that the energy harvesting and converting efficiency $\eta = 0.6$.

Fig.2 compares the users' achievable ergodic rates. The comparison scheme directly maximizes system's sum rate under the same constraints. We set two users, SIC capability as -80 dB and $N_t = N_r = 200$. It can be seen that with max-min optimizer, all users have same rates, which verifies that fairness is achieved between users. Although the sum-rate of the comparison scheme is higher, there are seriously unfairness between two users. Especially when P_d is small, since the optimizer allocates almost all the power to the user with better channel to achieve a higher sum-rate. Fig.2 also shows the performance of FD-WPCNs without energy beamforming, where the FD

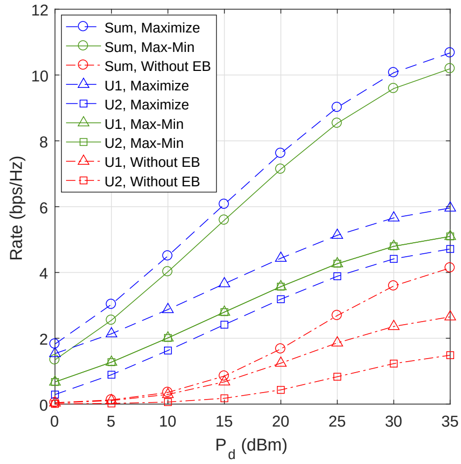

Figure 2: Comparison of achievable ergodic rate between 2 users.

HAP omni-directionally radiates energy. We can see that the achievable rate is much lower than the cases with energy beamforming. This is because without energy beamforming, most of the transmitted power is wasted during propagation. Moreover, there exists a performance gap between the two users, because it's hard for the user with the worse channel to harvest energy, which validates that energy beamforming can improve not only the rate performance of FD-WPCN systems but also among users.

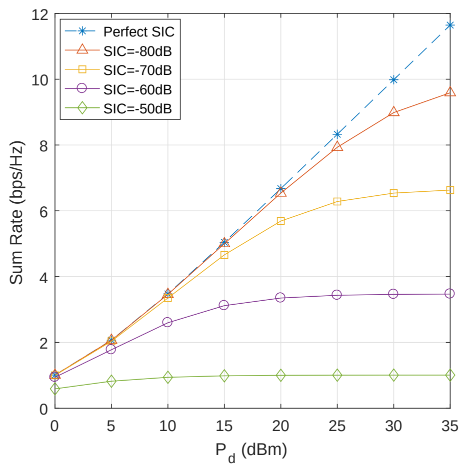

Figure 3: Sum rate versus WET power and residual SI with $K = 4$ and $N_t = N_r = 200$.

In Fig.3, we set four users and compare the schemes with different SIC capability. The ideal scheme with perfect SIC is also shown for comparison. It can be seen that with residual SI, the performance of the system is limited and the sum rate will converge to constant. It's obviously that with less residual SI, FD-WPCN can achieve higher sum rate with same P_d and converge slowly to higher upper bound. With -80 dB SIC capability, when $P_d < 20$ dBm, it can achieve almost same performance with ideal scheme, while with -50 dB SIC capability, the average sum-rate is limited under 1 bps/Hz, which may result in system's outage.

Further, with $N_t = N_r$, and fixed P_d = 30 dBm, Fig. 4 shows that the 1000 points simulation results match well with analytical lower bound derived in (17) for different number of users or antennas, which verifies that $\widetilde{R}_k$ matches well with R_k. It also shows that the sum rate increases with the increasing of N_t and N_r, so our FD-WPCN system can outperform other single-antenna schemes. What's more, the sum rate of FD-WPCN is improved when there are more users, while the users' rates decrease.

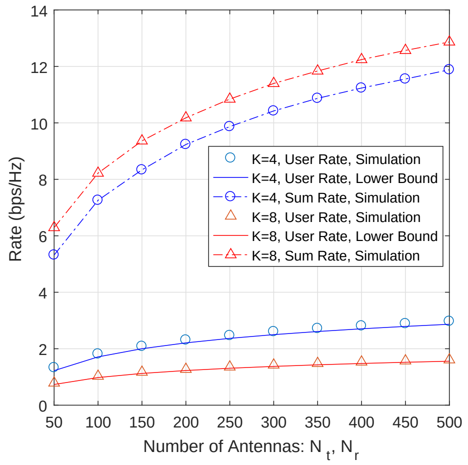

Figure 4: Comparison between analytical lower bound and Monte Carlo simulation results of achievable ergodic rates .

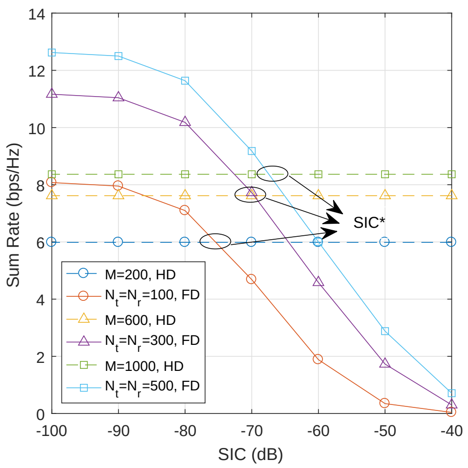

Figure 5: Sum rate comparison between FD-WPCN and HD-WPCN versus residual SI.

Finally, we compare the presented FD-WPCN's performance with HD-WPCN. The HD comparison scheme is according to [4], where the HAP is equipped with M antennas. One transmit block is divided into two phases, where in the first phase HAP allocates power to all users, and in the second phase all users uplink transmit information to HAP at the same time. To make a fair comparison, we use same beamformer as (2) in HD scheme, and the time of WET phase and WIT phase is set as $K\tau$ and τ, respectively. The number of antennas is set as $M = N_t + N_r$. Fig. 5 shows that with 4 users and fixed P_d = 30 dBm, FD-WPCN can outperform HD-WPCN in rates when SIC capability is better than a certain value (denoted by SIC^*). With $N_t = N_r = 100$, FD-WPCNs have better performance when SIC capability is better than -75 dB, which is easy to realize. In the proposed FD-WPCN system, the downlink transmit power is higher than that of conventional FD systems, which may result in higher residual SI. However, as discussed in Section 3, the SI can be effectively mitigated via the proposed energy beamforming technology. In other words, with energy beamforming with sufficient antennas, the proposed system can alleviate the higher residual SI caused by WET. From Fig. 5, with -75dB SIC capability, the system can achieve better performance than half-duplex systems when the number of antennas is greater than 200, which demonstrates that the residual SI is mitigated via energy beamforming.

6. Conclusion

This paper studies the effects of energy beamforming on FD-WPCNs with one full-duplex multi-antenna HAP and multiple single-antenna users. Using beamforming technology, we propose a space division energy allocation scheme and obtain each user's harvested energy in the downlink. To analyse users' performance, we derive an approximate expression of users' achievable ergodic rate as a function of residual SI and the number of antennas. We further optimize the energy allocation under the max-min fairness constraint to ensure fairness among users, and derive a closed-form solution. Numerical and simulation results have been provided to demonstrate the effects of beamforming on improving rates and fairness, and suppressing SI, and indicate that FD technology together with beamforming technology has potential to further bring benefits to WPCNs.

Acknowledgments

This work was supported in part by National Natural Science Foundation of China (61771358), Intergovernmental International Cooperation on Science and Technology Innovation (2016YFE0122900), and the 111 Project (B08038).

References

[1] H. Tabassum, E. Hossain, A. Ogundipe, I. K. Dong, Wireless-powered cellular networks: key challenges and solution techniques, Communications Magazine IEEE 53 (2015) 63–71.

[2] N. Zhao, F. R. Yu, V. C. M. Leung, Opportunistic communications in interference alignment networks with wireless power transfer, IEEE Wireless Communications 22 (2015) 88–95.

[3] D. Hwang, I. K. Dong, T. J. Lee, Throughput maximization for multiuser mimo wireless powered communication networks, IEEE Transactions on Vehicular Technology 65 (2016) 5743–5748.

[4] G. Yang, C. K. Ho, R. Zhang, Y. L. Guan, Throughput optimization for massive mimo systems powered by wireless energy transfer, IEEE Journal on Selected Areas in Communications 33 (2014) 1640–1650.

[5] K. Liang, L. Zhao, K. Yang, X. Chu, Online power and time allocation in mimo uplink transmissions powered by rf wireless energy transfer, IEEE Transactions on Vehicular Technology PP (2017) 1–1.
[6] N. Zhao, F. R. Yu, V. C. M. Leung, Wireless energy harvesting in interference alignment networks, Communications Magazine IEEE 53 (2015) 72–78.
[7] J. Guo, N. Zhao, F. R. Yu, X. Liu, V. C. M. Leung, Exploiting adversarial jamming signals for energy harvesting in interference networks, IEEE Transactions on Wireless Communications 16 (2017) 1267–1280.
[8] H. Tabassum, E. Hossain, On the deployment of energy sources in wireless-powered cellular networks, IEEE Transactions on Communications 63 (2015) 3391–3404.
[9] X. Kang, C. K. Ho, S. Sun, Full-duplex wireless-powered communication network with energy causality, IEEE Transactions on Wireless Communications 14 (2015) 5539–5551.
[10] H. Ju, R. Zhang, Optimal resource allocation in full-duplex wireless-powered communication network, Communications IEEE Transactions on 62 (2014) 3528–3540.
[11] Y. Li, P. Fan, A. Leukhin, L. Liu, On the spectral and energy efficiency of full-duplex small-cell wireless systems with massive mimo, IEEE Transactions on Vehicular Technology 66 (2017) 2339–2353.
[12] B. K. Chalise, H. A. Suraweera, G. Zheng, G. K. Karagiannidis, Beamforming optimization for full-duplex wireless-powered mimo systems, IEEE Transactions on Communications PP (2017) 1–1.
[13] J. Xu, L. Liu, R. Zhang, Multiuser miso beamforming for simultaneous wireless information and power transfer, IEEE Transactions on Signal Processing 62 (2014) 4798–4810.
[14] Z. Sun, L. Dan, Y. Xiao, P. Yang, S. Li, Energy borrowing for energy harvesting wireless communications, IEEE Communications Letters 20 (2016) 2546–2549.
[15] J. Fan, Z. Xu, G. Y. Li, Performance analysis of mu-mimo in downlink cellular networks, IEEE Communications Letters 19 (2015) 223–226.
[16] H. Q. Ngo, E. G. Larsson, T. L. Marzetta, Energy and spectral efficiency of very large multiuser mimo systems, IEEE Transactions on Communications 61 (2011) 1436–1449.
[17] J. M. Bernardo, A. F. M. Smith, Bayesian Theory, 2008.